Supplementary data

Structure-DFT-Bioactivity Correlation in Mixed-Ligand Fe(III), Mn(II), and V(IV)O Complexes with Bidentate NO Donors 1H-benzimidazole-2-carboxylic acid and Norfloxacin Ligands

Hany M. Abd El-Lateef[1*], Mai M. Khalaf[1*], Aly Abdou[2*]

[1]Department of Chemistry, College of Science, King Faisal University, Al-Ahsa 31982, Saudi Arabia

[2]Department of Chemistry, Faculty of Science, Sohag University, Sohag 82524, Egypt

* Corresponding authors: hmahmed@kfu.edu.sa (H. M. Abd El-Lateef.); aly_abdou@science.sohag.edu.eg (A. Abdou)

S. 1. Materials

The materials used in this study were of analytical reagent grade. These included iron(III) chloride hexahydrate ($FeCl_3 \cdot 6H_2O$), manganese (II) chloride dihydrate ($MnCl_2 \cdot 2H_2O$), oxovanadium(IV) acetylacetonate [$VO(acac)_2$], norfloxacin, and 1H-benzimidazole-2-carboxylic acid, along with organic solvents such as ethanol, dimethyl sulfoxide, and dimethylformamide.

S. 2.1.3. Structural Characterization

Elemental analyses for carbon, hydrogen, and nitrogen were carried out using a PerkinElmer 2408 elemental analyzer, while the metal content was determined by atomic absorption spectroscopy using a PerkinElmer 2380 instrument. Infrared spectra were recorded on a Bruker FT-IR spectrometer (model 8101) in the range 4000-400 cm^{-1} to identify functional groups and metal-ligand coordination modes. Electronic absorption spectra were measured using a Jasco V-750 UV-Vis spectrophotometer for 10^{-3} mol L^{-1} solutions, providing information on ligand-centered and metal-centered transitions. Mass spectrometric analyses were performed using a Thermo Scientific ISQ gas chromatography-mass spectrometry system equipped with a direct inlet probe and operating under electron ionization conditions, enabling confirmation of molecular weights and fragmentation patterns. Thermal behavior of the ligands and complexes was investigated by thermogravimetric and differential thermal analyses using a Shimadzu thermal analyzer (model 60H) at a heating rate of 10 °C min^{-1} under an inert atmosphere, allowing assessment of thermal stability and the presence of coordinated or lattice solvent molecules. Molar conductance measurements were carried out at room temperature using a Jenway conductivity meter (model 4320) for 10^{-3} mol L^{-1} solutions in dimethylformamide to evaluate the electrolytic nature of the complexes. Magnetic susceptibility measurements of powdered samples were performed using a Bartington magnetic susceptibility balance, and the effective

magnetic moments were calculated to support the proposed geometries and electronic configurations. In addition, the spectrophotometric continuous variation (Job's) method was employed to determine the metal-to-ligand stoichiometry of the synthesized complexes in solution.

S.2. Stoichiometry of the synthesized mixed-ligand complexes

The continuous variation method was used to establish the composition of the ternary M : BC: NR) complexes [1, 2]. The molar fractions of two of the components were varied continuously, keeping their total concentration constant in the presence of a large excess of the third component. Under these conditions, the ternary system was modified to a pseudo-binary system [1, 2].

Firstly, for determination of the stoichiometry of M: BC in the presence of NR as mixed ligands. A series of solutions containing different ratios of M:BC, were prepared (in the presence of an excess of NR), keeping the total concentration of both M ion and BC constant. The ratio of M:BC, was determined from the relationship between absorbance (Abs) (at the λ_{max} of the target complex) and mole fraction of BC (BC/(BC+M)).

Secondly, the ratio of M:NR was determined as described above in the presence of excess (BC). A series of solutions containing different ratios of M:NR, were prepared (in the presence of an excess of BC), keeping the total concentration of both M ion and NR constant. The ratio of M:NR, was determined from the relationship between absorbance (Abs) (at the λ_{max} of the target complex) and mole fraction of NR (NR/(NR+M)).

The results proved the 1:1:1 (M:BC:NR.) ternary complexes were formed for FeBCNR, MnBCNR and VOBCNR complexes.

S.3. DFT calculation

The global reactivity descriptors, ionization potential (IP), electron affinity (EA), energy gap (ΔE), electronegativity (χ), chemical potential (μ), chemical hardness (η), softness (σ), electrophilicity index (ω), and nucleophilicity (Nu), were calculated using Eqns. 1-9 [35-37].

$IP=-E_{HOMO}$	equation (1)
$EA=-E_{LUMO}$	equation (2)
$\Delta E = IP - EA$	equation (3)
$X=-[E_{LUMO}+E_{HOMO}]/2$	equation (4)
$\mu=(E_{HOMO}+E_{LUMO})/2$	equation (5)
$\eta=-[E_{LUMO}-E_{HOMO}]/2$	equation (6)
$\sigma=1/\eta$	equation (7)
$\omega=\mu^2/2\eta$	equation (8)
$Nu = 1/\omega$	equation (9)

S.4. Biological Activity

In Vitro antimicrobial activity

In Vitro Antibacterial activity

The *in vitro* antibacterial activities of the understudy compounds were evaluated against two Gram-positive bacterial strains (***B. subtilis***, and ***S. aureus***), and two Gram-negative bacteria strains (***E. coli***, and ***K. pneumoniae***) using the disk diffusion method [3]. A 100 µL suspension of each bacterium, containing approximately 0.5×10^6 CFU, was evenly spread onto Muller Hinton Agar plates using a sterile swab. The compounds were dissolved in DMSO at a concentration of 1.5 mg/mL, and sterile discs (6 mm in diameter) were impregnated with the solutions and placed on the inoculated agar surface. The plates were inverted and incubated at 37 °C for 24 hours. As the samples diffused, bacterial growth was inhibited around the discs. After incubation, the antibacterial efficacy was assessed by measuring the diameter of the inhibition zones in millimeters. DMSO, serving as the solvent, showed no effect on bacterial growth and was used as a negative control.

***In Vitro* Aantifungal activity**

The antifungal activity screening was conducted using the disk diffusion method. The antifungal properties of the ligand and its complexes were tested against two fungal strains, ***C. albicans***, and ***A. niger***. In this procedure, discs were soaked in compound solutions at a concentration of 1.5 mg/mL in DMSO and placed at various positions on Sabouraud Dextrose Agar plates inoculated with fungal spore suspensions (10^5 CFU/mL) [4]. The plates with ***C. albicans***, and ***A. niger*** were incubated at 32 °C for 24 hours and 37 °C for 7 days, respectively. Following incubation, the inhibition zones (measured in millimeters) formed around each disc was recorded to assess the antifungal activity of the compounds.

Activity Index (%)

The effectiveness of the antibiotic amoxicillin and the antifungal agent clotrimazole was also evaluated using the same methods to determine their efficacy as standard antibacterial and antifungal agents against the tested microorganisms. The % Activity Index was calculated by dividing the inhibition zone (IZ) of the test compound by the IZ of the standard drug and multiplying by 100 [5]. This comparison provided a comprehensive assessment of the antibacterial and antifungal activities of the compounds in relation to the standard drugs, amoxicillin and clotrimazole.

Minimum inhibitory concentration (MIC)

The Minimum Inhibitory Concentrations (MIC) were determined using the broth dilution method. In this procedure, each sample was dissolved in DMSO at various concentrations ranging from 10.0 to 200 μM under sterile conditions. To each tube containing the sample, 650 μL of Muller Hinton Broth and 100 μL of the tested microorganism were added. The tubes were then incubated at 37 °C for 24 hours. The MIC was defined as the lowest concentration of the antibacterial sample that inhibited visible microbial growth, as indicated by the absence of turbidity in the mixture [6].

Anti-inflammatory activity

In an *in vitro* study, the anti-inflammatory effectiveness of the title products was assessed via evaluating their ability to reduce the denaturation of egg albumin (protein) [7, 8]. To conduct the experiment, a reaction mixture of five milliliters was organized via combining 0.2 milliliter of egg albumin solution (derived from fresh hen's eggs), 2 milliliters of the title components (or the standard drug Ibuprofen) at varying concentrations, and 2.8 milliliter of phosphate-buffered saline (pH 7.4). The final concentrations of the title components were adjusted to 10, 50, 100, 250, and 500 μM. As a control, a separate mixture of five milliliters was created via mixing 0.2 milliliters of egg albumin solution, two milliliters of bi-distilled water, and 2.8 milliliter of phosphate-buffered saline. Both sets of mixtures were incubated at thirty-seven °C for thirty minutes and then heated in a water bath at seventy °C for fifteen minutes. After cooling, the absorbance of each mixture was measured at 660 nm using a UV-Vis spectrophotometer, with bi-distilled water serving as the blank. The percentage inhibition of protein denaturation was calculated using the formula: $\%\,\text{inhibition} = \frac{A_c - A_t}{A_c} \times 100$, where at represents the absorbance of the test sample and Ac represents the absorbance of the control. The experiments were conducted in triplicate, with ibuprofen serving as the standard component. Additionally, the concentration of the title components or the standard drug that caused 50% inhibition (IC_{50}) was determined using https://www.aatbio.com/tools/ic50-calculator.

S.5. Molecular docking

The molecular docking studies for the investigated compounds were performed using AutoDock Vina [9]. The crystal structures of two target proteins were selected for this analysis: the 24 kDa ATPase domain of *E. coli* DNA Gyrase B in complex with 1-ethyl-3-[8-methyl-5-(2-methyl-pyridin-4-yl)-isoquinolin-3-yl]-urea (PDB ID: 5MMN) [10], obtained from the Protein Data Bank (PDB, https://www.rcsb.org/). Prior to docking, the receptors were prepared by removing water molecules, ligands, and heteroatoms, followed by the addition of polar hydrogen atoms and Kollman charges to optimize the proteins. The ligands were initially designed using chemsketch, converted into PDBQT format after energy minimization. The docking grid boxes were carefully defined with the following coordinates: (X = -41.573, Y = 9.665, Z = 8.566) for 5MMN. The binding energies of the compounds were computed to assess their affinities for the target proteins, offering valuable insights into ligand-protein interactions.

The choice of PDB ID 5MMN for molecular docking studies was a strategic decision to investigate novel compounds targeting clinically significant enzyme. PDB ID 5MMN corresponds to the *E. coli* DNA Gyrase B 24 kDa ATPase domain bound to a specific inhibitor, serving as an essential target in antibacterial drug development. DNA gyrase plays a pivotal role in bacterial DNA replication, and its inhibition provides a promising strategy to address bacterial infections [10]. This well-characterized protein structure enables molecular docking studies to uncover potential antibacterial agents, highlighting their versatility and therapeutic value in addressing diverse disease conditions.

Table (S.1): Physical properties of the (BC, NR ligands) and (FeBCNR, MnBCNR, and VOBCNR complexes)					
	ligands		**Complexes**		
	BC	**NR**	**FeBCNR**	**MnBCNR**	**VOBCNR**
Color		white	Brownish red	pale pink	pale green
Melting point (°C)		220	> 300	> 300	> 300
Yield (%)	----	----	80	81	80

Table (S.2): Elemental analysis found (calculated) % of the (FeBCNR, MnBCNR, and VOBCNR complexes)					
	ligands		**Complexes**		
	BC	**NR**	**FeBCNR**	**MnBCNR**	**VOBCNR**
C	----	----	4.22 (4.96)	50.01 (50.53)	53.29 (52.76)
H	----	----	4.86 (4.11)	5.15 (4.59)	4.88 (4.06)
N	----	----	12.35 (11.89)	11.66 (12.28)	13.34 (12.82)
M	----	----	10.11 (9.49)	10.28 (9.63)	9.86 (9.32)

Table (S.3): Effective Magnetic moment (μ_{eff} (B.M)) of the (FeBCNR, MnBCNR, and VOBCNR complexes)				
ligands		**Complexes**		
BC	**NR**	**FeBCNR**	**MnBCNR**	**VOBCNR**
----	----	1.86	1.81	1.77

Table (S.4): conductivity of the (FeBCNR, MnBCNR, and VOBCNR complexes) in Ethanol					
	ligands		**Complexes**		
	BC	**NR**	**FeBCNR**	**MnBCNR**	**VOBCNR**
μ_v, $\Omega^{-1}cm^2mol^{-1}$	----	----	9.85	9.03	9.42

Table (S.5): Calculated frontier orbital energies (HOMO and LUMO), energy gap (ΔE), ionization potential (IP), electron affinity (EA), electronegativity (χ), chemical potential (μ), chemical hardness (η), softness (σ), electrophilicity index (ω), and nucleophilicity index (Nu), all expressed in eV, derived from HOMO-LUMO energies.

	HOMO	LUMO	ΔE	IP	EA	χ	μ	η	σ	ω	Nu
BC	-7.03	-2.09	4.94	7.03	2.09	4.56	-4.56	2.47	0.20	4.21	0.24
NR	-5.86	-1.73	4.13	5.86	1.73	3.80	-3.80	2.07	0.24	3.48	0.29
FeBCNR	-4.87	-2.11	2.76	4.87	2.11	3.49	-3.49	1.38	0.36	4.41	0.23
MnBCNR	-6.14	-2.74	3.39	6.14	2.74	4.44	-4.44	1.70	0.29	5.81	0.17
VOBCNR	-5.26	-2.27	2.99	5.26	2.27	3.77	-3.77	1.49	0.33	4.75	0.21

Table (S.6): Antibacterial activity as diameter of zone inhibition in mm

	Diameter of zone inhibition in mm			
	Gram-positive bacteria		**Gram-negative bacteria**	
	B. subtilis	***S. aureus***	***E. coli***	***K. pneumoniae***
BC	9 ±0.18	9 ±0.14	8 ±0.12	9 ±0.12
NR	11 ±0.15	11 ±0.15	11 ±0.13	10 ±0.11
FeBCNR	28 ±0.09	28 ±0.18	23 ±0.14	25 ±0.12
MnBCNR	27 ±0.11	28 ±0.11	21 ±0.12	24 ±0.13
VOBCNR	28 ±0.12	28 ±0.13	22 ±0.11	25 ±0.13
Amoxicillin	30 ±0.10	30 ±0.12	25 ±0.11	28 ±0.12

Table (S.7): Antibacterial activity as Activity index (%)

	Activity index (%)			
	Gram-positive bacteria		**Gram-negative bacteria**	
	B. subtilis	***S. aureus***	***E. coli***	***K. pneumoniae***
BC	30.00 ±0.42	30.00 ±0.38	32.00 ±0.33	32.14 ±0.32
NR	36.67 ±0.33	36.67 ±0.24	44.00 ±0.27	35.71 ±0.40
FeBCNR	93.33 ±0.35	93.33 ±0.33	92.00 ±0.30	89.29 ±0.34
MnBCNR	90.00 ±0.34	93.33 ±0.28	84.00 ±0.28	85.71 ±0.37
VOBCNR	93.33 ±0.40	93.33 ±0.30	88.00 ±0.25	89.29 ±0.30
Amoxicillin	100	100	100	100

Table (S.8): Anti-fungal activity as diameter of zone inhibition in mm		
	Diameter of zone inhibition in mm	
Comp.	***C. albicans***	***A. niger***
BC	9 ±0.14	9 ±0.30
NR	10 ±0.21	10 ±0.27
FeBCNR	19 ±0.19	16 ±0.31
MnBCNR	17 ±0.31	16 ±0.22
VOBCNR	18 ±0.21	16 ±0.24
clotrimazole	20 ±0.11	18 ±0.18

Table (S.9): Anti-fungal activity as Activity index (%)		
	Activity index (%)	
Comp.	***C. albicans***	***A. niger***
BC	9 ±0.34	9 ±0.28
NR	10 ±0.40	10 ±0.24
FeBCNR	19 ±0.28	16 ±0.30
MnBCNR	17 ±0.28	16 ±0.29
VOBCNR	18 ±0.30	16 ±0.31
clotrimazole	100	100

Table (S.10): Antibacterial and Antifungal activity as Minimum Inhibition Concentration (MIC, μM)						
Comp. No	**Minimal Inhibitory Concentration (MIC) in μM**					
	Gram-positive bacteria		**Gram-negative bacteria**		**Fungi**	
	B. subtilis	***S. aureus***	***E. coli***	***K. pneumoniae***	***C. albicans***	***A. niger***
BC	120 ±0.34	120 ±0.32	120 ±0.30	120 ±0.31	120 ±0.24	120 ±0.30
NR	100 ±0.31	100 ±0.42	100 ±0.28	100 ±0.28	100 ±0.31	100 ±0.25
FeBCNR	80 ±0.32	80 ±0.32	70 ±0.31	70 ±0.31	80 ±.28	80 ±0.27
MnBCNR	90 ±0.22	80 ±0.33	80 ±0.31	80 ±0.25	80 ±0.31	80 ±0.30
VOBCNR	80 ±0.35	80 ±0.41	80 ±0.33	70 ±0.33	80 ±0.27	80 ±0.34

Table (S.11): Anti-inflammatory results as Mean percentage inhibition (%), and Half-maximal Inhibitory Concentration (IC_{50}).						
	Percentage of Inhibition (%)					
Concentration (μM)	BC	NR	FeBCNR	MnBCNR	VOBCNR	Standard
10	3.00 ±0.38	5.00 ±0.33	8.00 ±0.28	10.33 ±0.31	11.33 ±0.34	19.78 ±0.22
50	11.00 ±0.36	14.33 ±0.35	22.00 ±0.26	30.33 ±0.27	32.33 ±0.22	46.86 ±0.31
100	28.67 ±0.40	33.67 ±0.28	55.00 ±0.31	65.33 ±0.22	67.67 ±0.30	76.82 ±0.25
250	61.67 ±0.27	68.00 ±0.34	92.00 ±0.28	95.00 ±0.36	96.00 ±0.25	81.18 ±0.31
500	87.67 ±0.37	90.67 ±0..31	97.00 ±0.31	99.33 ±0.30	99.00 ±0.20	82.28 ±0.24
IC_{50} μM	222.169 ±0.37	182.8076 ±0.31	96.6407 ±0.24	82.913 ±0.26	79.7619 ±0.31	53.47 ±0.26

Table (S.12): Interactions of the studied compounds and the amino acids residues of the target DNA gyrase B (PDB: 5MMN).				
	Residues	Distance	Interaction	Binding energy (Kcal/mol)
BC	ASP73	2.24	Hydrogen Bond	-6.10
	ARG76	5.31	Electrostatic	
	ALA47	4.87	Hydrophobic	
	VAL167	5.44	Hydrophobic	
NR	GLU50	4.46	Electrostatic	-6.90
	VAL43	3.46	Hydrogen Bond	
	GLU50	2.70	Hydrogen Bond	
	GLU50	2.60	Hydrogen Bond	
	GLU50	3.13	Halogen	
	ILE78	3.28	Hydrophobic	
	ILE94	3.73	Hydrophobic	
	ILE78	4.37	Hydrophobic	
FeCBNR	ASP73	4.37	Electrostatic	-8.60
	ASP73	2.36	Hydrogen Bond	
	VAL43	2.65	Hydrogen Bond	
	GLU50	2.77	Hydrogen Bond	
	ASN46	3.56	Halogen	
	ILE78	3.80	Hydrophobic	
	ILE94	5.27	Hydrophobic	
MnCBNR	ASP49	5.14	Electrostatic	-7.90
	ASN46	2.32	Hydrogen Bond	
	ASP49	4.97	Electrostatic	
	PRO79	5.30	Hydrophobic	
VOCBNR	GLU50	5.04	Electrostatic	-8.40
	ARG136	1.94	Hydrogen Bond	
	ARG76	3.16	Halogen	
	ARG76	4.10	Electrostatic	
	PRO79	4.60	Hydrophobic	
	PRO79	4.42	Hydrophobic	
	ILE78	4.74	Hydrophobic	
chloramphenicol	VAL43	3.53	Hydrogen bond	-9.00
	ALA47	3.35	Hydrogen bond	
	ILE78	3.54	Hydrogen bond	
	PRO79	3.66	Hydrogen bond	
	ILE78	3.68	Hydrophobic	

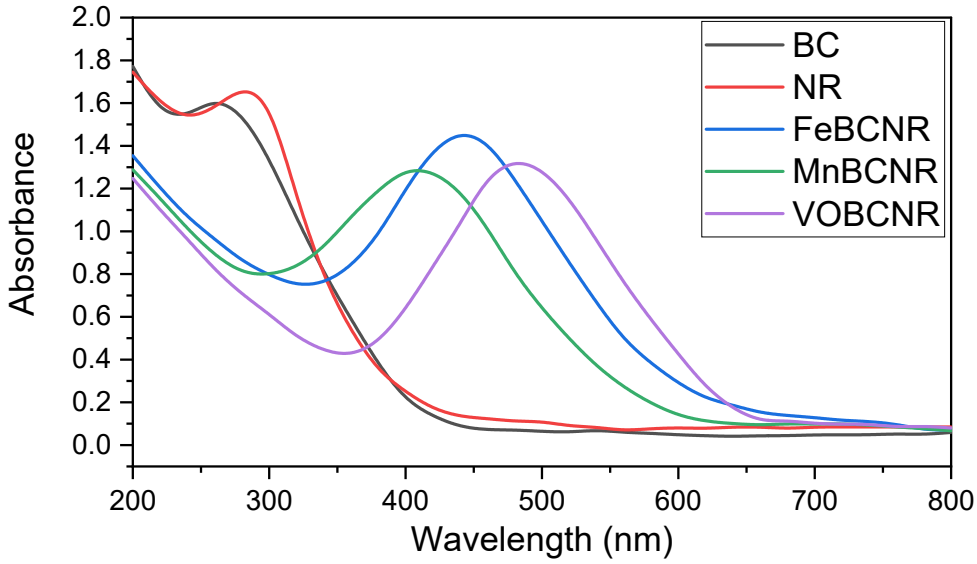

Fig. (S.1): The UV-vis. spectra of the (BC, NR ligands) and (FeBCNR, MnBCNR, and VOBCNR complexes)

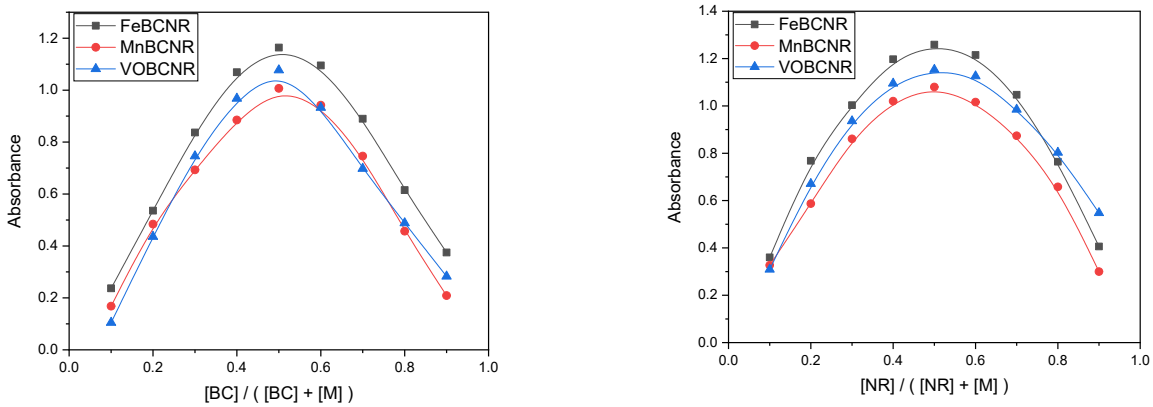

Fig. (S.2): The Stiochiometry of the (FeBCNR, MnBCNR, and VOBCNR complexes

FeBCNR

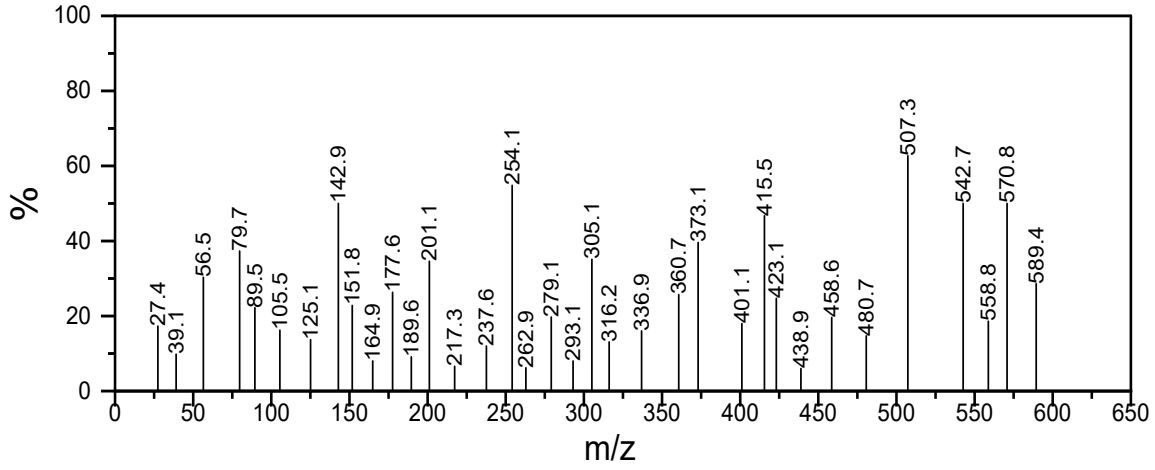

MnBCNR

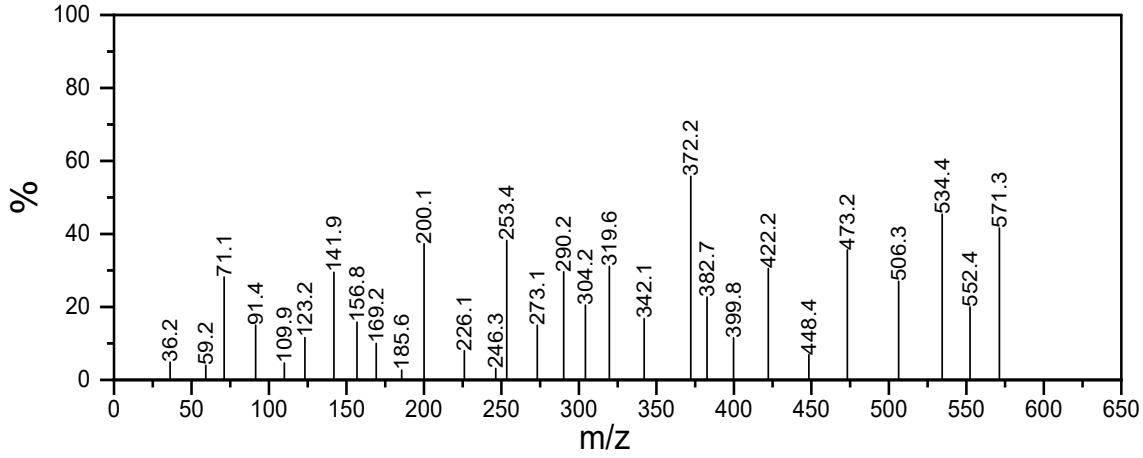

VOBCNR

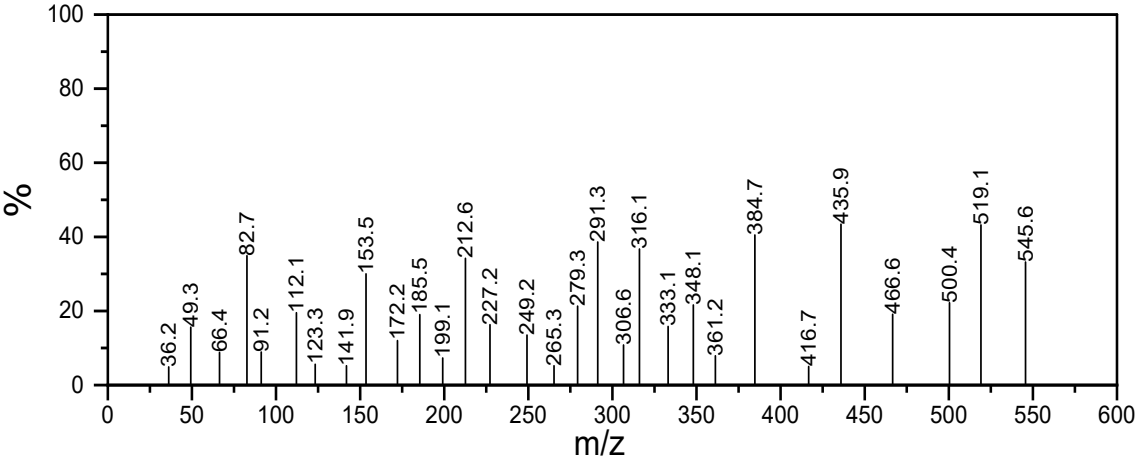

Fig. (S.3): Mass spectra of the FeBCNR, MnBCNR, and VOBCNR

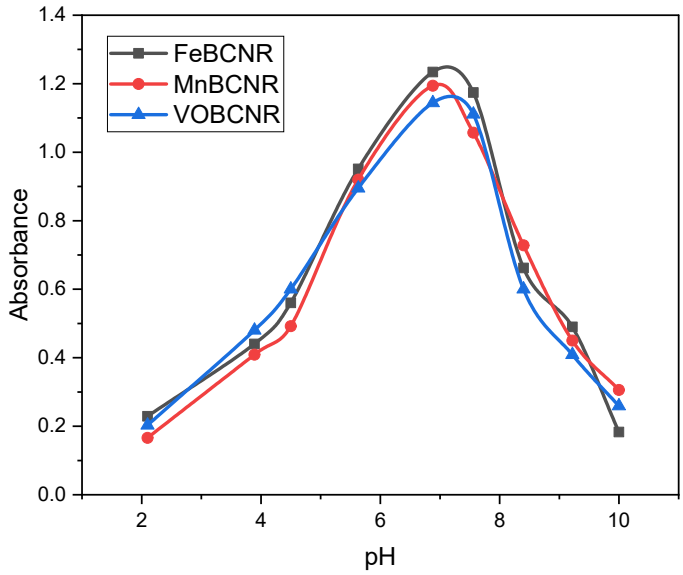

Fig. (S.4): pH stability curve of the FeBCNR, MnBCNR, and VOBCNR complexes.

BC

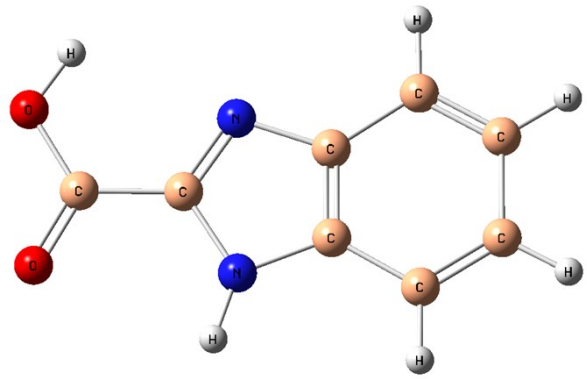

NR

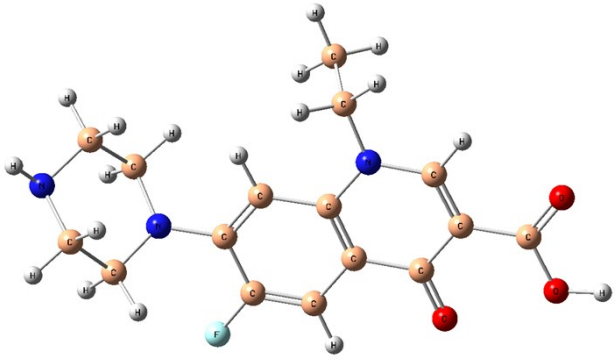

FeBCNR

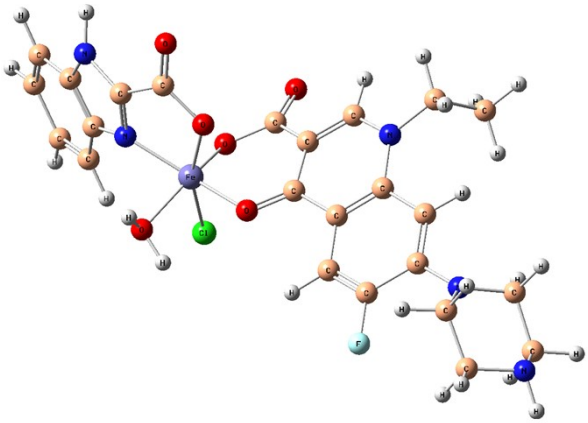

MnBCNR

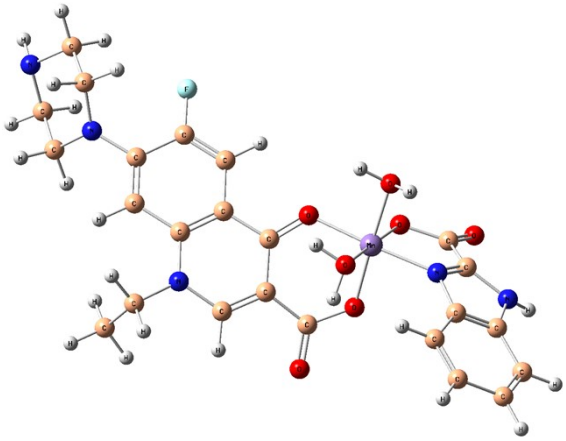

VOBCNR

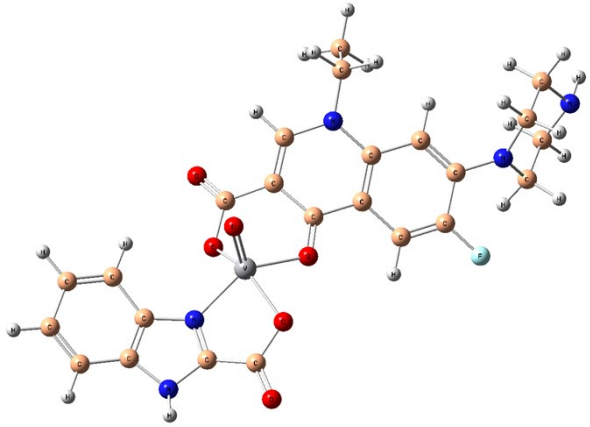

Fig. (S.5): Optimized 3D structures of (FeBCNR, MnBCNR, and VOBCNR complexes

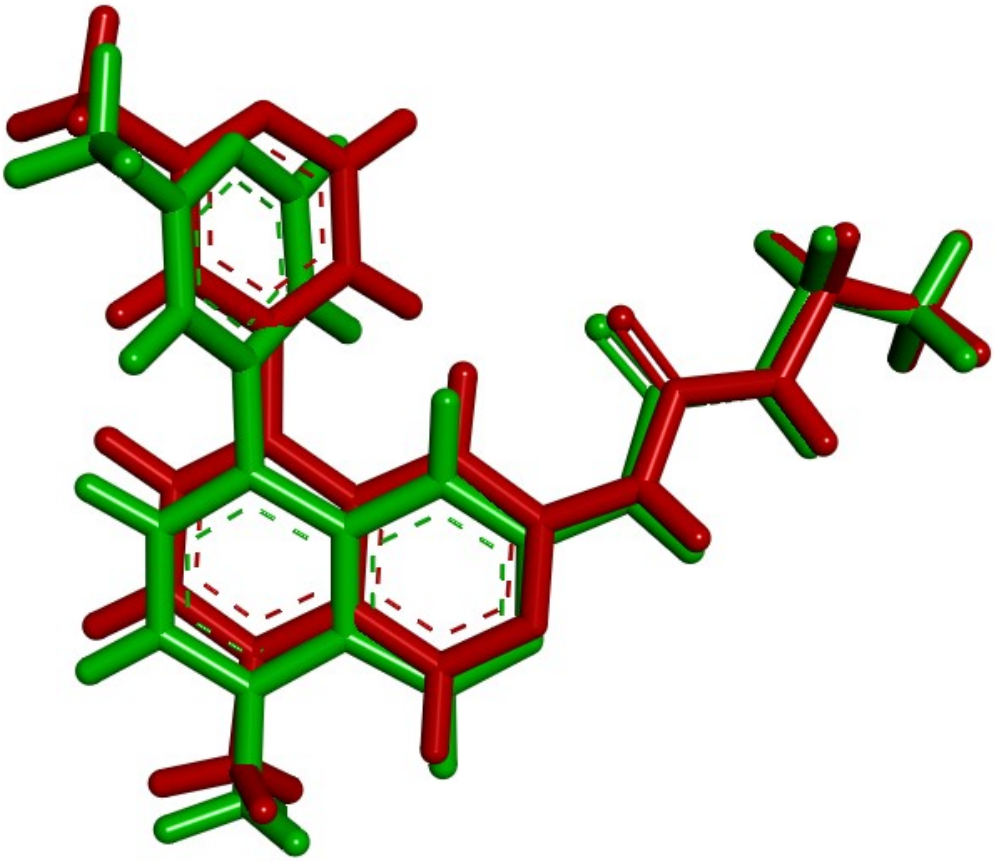

Fig. (S.6): 3D of the superimposition of the co-crystallized (Red) and the redocking pose (blue) of the 1-ethyl-3-[8-methyl-5-(2-methylpyridin-4-yl)isoquinolin-3-yl]urea ligand in DNA gyrase B (PDB: 5MMN)

References

[1] A. Gahlan, M. El-Mottaleb, N. Badawy, F. Kamale, S.H. Ali, Spectrophotometeric studies on binary and ternary complexes of some metal ions with alizarin red S and cysteine, Int. J. Adv. Res 2(10) (2014) 570-584.

[2] R.M. El-Khatib, L.A.-M.E. Nassr, Spectrophotometric study of some Mn (II) ternary complexes and their analytical applications, Monatshefte für Chemie-Chemical Monthly 140 (2009) 1139-1142.

[3] M. Mackeen, A. Ali, S. El-Sharkawy, M. Manap, K. Salleh, N. Lajis, K. Kawazu, Antimicrobial and cytotoxic properties of some Malaysian traditional vegetables (ulam), Int. J. Pharm. 35(3) (1997) 174-178.

[4] N. Raman, A. Sakthivel, K. Rajasekaran, Synthesis and spectral characterization of antifungal sensitive Schiff base transition metal complexes, Mycobiology 35(3) (2007) 150-153.

[5] A.D. Kulkarni, S.A. Patil, P.S. Badami, Electrochemical properties of some transition metal complexes: synthesis, characterization and in-vitro antimicrobial studies of Co (II), Ni (II), Cu (II), Mn (II) and Fe (III) complexes, International Journal of Electrochemical Science 4(5) (2009) 717-729.

[6] I. Wiegand, K. Hilpert, R.E. Hancock, Agar and broth dilution methods to determine the minimal inhibitory concentration (MIC) of antimicrobial substances, Nat. Protoc. 3(2) (2008) 163-175.

[7] A.M. El-Saghier, S.S. Enaili, A. Abdou, A.M. Hamed, A.M. Kadry, An operationally simple, one-pot, convenient synthesis, and in vitro anti-inflammatory activity of some new spirotriazolotriazine derivatives, J. Heterocycl. Chem. 61(1) (2024) 146-162.

[8] H.M. Abd El-Lateef, M.M. Khalaf, A.A. Amer, A.A. Abdelhamid, A. Abdou, Antibacterial, antifungal, anti-inflammatory evaluation, molecular docking, and density

functional theory exploration of 2-(1H-benzimidazol-2-yl)guanidine mixed-ligand complexes: Synthesis and characterization, Appl. Organomet. Chem. 38(1) (2024) e7299.

[9] O. Trott, A.J. Olson, AutoDock Vina: improving the speed and accuracy of docking with a new scoring function, efficient optimization, and multithreading, Journal of computational chemistry 31(2) (2010) 455-461.

[10] F. Jalali-Yazdi, S. Chowdhury, C. Yoshioka, E. Gouaux, Mechanisms for zinc and proton inhibition of the GluN1/GluN2A NMDA receptor, Cell 175(6) (2018) 1520-1532. e15.

[11] R.G. Kurumbail, A.M. Stevens, J.K. Gierse, J.J. McDonald, R.A. Stegeman, J.Y. Pak, D. Gildehaus, J.M. Iyashiro, T.D. Penning, K. Seibert, Structural basis for selective inhibition of cyclooxygenase-2 by anti-inflammatory agents, Nature 384(6610) (1996) 644-648.